

Multi-modal Integration Analysis of Alzheimer's Disease Using Large Language Models and Knowledge Graphs

Kanan Kiguchi¹, Yunhao Tu², Katsuhiko Ajito¹, Fady Alnajjar^{3*}, Kazuyuki Murase¹

¹Department of Information Technology, Faculty of Information Science and Technology, International Professional University of Technology in Osaka (IPUT Osaka), 3-3-1 Umeda, Kita-ku, Osaka-shi, Osaka 530-0001, Japan

²Department of Computer Science, College of Engineering, Chubu University, 1200 Matsumoto-cho, Kasugai-shi, Aichi 487-8501, Japan

³College of Information Technology, United Arab Emirates University (UAEU), Al Ain, Abu Dhabi, United Arab Emirates

*Corresponding author: Fady Alnajjar (e-mail: fady.alnajjar[at]uaeu.ac.ae).

This work was supported by IPUT Osaka for KA and KM, the Nitto Foundation, the Chubu University Grant K, and JSPS KAKENHI for YT, as well as by the UAEU for FA

ABSTRACT We propose a novel framework for integrating fragmented multi-modal data in Alzheimer's disease (AD) research using large language models (LLMs) and knowledge graphs. While traditional multimodal analysis requires matched patient IDs across datasets, our approach demonstrates population-level integration of MRI, gene expression, biomarkers, EEG, and clinical indicators from independent cohorts. Statistical analysis identified significant features in each modality, which were connected as nodes in a knowledge graph. LLMs then analyzed the graph to extract potential correlations and generate hypotheses in natural language. This approach revealed several novel relationships, including a potential pathway linking metabolic risk factors to tau protein abnormalities via neuroinflammation ($r>0.6$, $p<0.001$), and unexpected correlations between frontal EEG channels and specific gene expression profiles ($r=0.42-0.58$, $p<0.01$). Cross-validation with independent datasets confirmed the robustness of major findings, with consistent effect sizes across cohorts (variance $<15\%$). The reproducibility of these findings was further supported by expert review (Cohen's $\kappa=0.82$) and computational validation. Our framework enables cross modal integration at a conceptual level without requiring patient ID matching, offering new possibilities for understanding AD pathology through fragmented data reuse and generating testable hypotheses for future research.

INDEX TERMS Alzheimer’s Disease, Biomarker, Clinical Diagnosis, Cross-modal analysis, EEG, Gene Expression, Hypothesis, Knowledge Graph, Large Language Model, MRI, Multi-modal Data

I. INTRODUCTION

Alzheimer’s disease (AD) represents one of the most significant healthcare challenges of the 21st century, affecting over 55 million people globally and projected to triple by 2050 [1]. This progressive neurodegenerative disorder manifests through a complex interplay of pathological processes that begin decades before clinical symptoms emerge. Early stages are marked by molecular alterations, including amyloid- β accumulation and tau hyperphosphorylation, followed by structural brain changes, functional alterations in neural networks, and eventually cognitive decline [2,3]. Understanding this complicated cascade of events requires integrating diverse types of data across multiple biological scales and measurement modalities—a challenge that has persistently hampered comprehensive AD research.

The multifaceted nature of AD pathophysiology necessitates approaches that can simultaneously analyze molecular, structural, functional, and clinical dimensions of the disease. Recent advances in neuroimaging, molecular biomarkers, electrophysiological measurements, and computational methods have generated unprecedented volumes of AD-related data [4]. However, these advances have paradoxically created a significant challenge: the fragmentation of knowledge across disconnected datasets and research silos, making it difficult to form a cohesive understanding of the disease.

Magnetic Resonance Imaging (MRI) studies have consistently revealed significant atrophy in specific brain regions in AD, particularly the hippocampus and medial temporal lobe [5,6]. Volumetric measurements and cortical thickness analyses using structural MRI can detect these changes even in early disease stages, with several longitudinal studies demonstrating that the rate of brain atrophy correlates closely with cognitive decline and disease progression [7].

Complementing these structural insights, Electroencephalography (EEG) provides critical information about functional brain changes in AD that often goes unexplored in isolation. EEG recordings have identified alterations in brain electrical activity, particularly slowing of rhythms with reductions in alpha/beta power and increases in delta/theta activity [8,9]. These functional changes often precede structural alterations visible on MRI, suggesting potential for earlier diagnosis—a critical need in a field where

treatment efficacy depends heavily on early intervention. Recent advances in EEG analysis techniques, including connectivity measures and machine learning approaches, have improved detection of subtle network reorganization patterns that may characterize incipient AD [9].

Meanwhile, molecular biomarkers and genetic data provide essential insights into underlying biological mechanisms driving disease progression [10], yet these datasets rarely connect directly with neuroimaging or clinical information from the same patients. The integration of these measurement types—structural, functional, and molecular—offers particularly valuable insights into AD pathophysiology by connecting observations across different biological scales.

A. Prior Work in Multimodal AD Data Integration

Previous approaches to multimodal AD data integration have predominantly relied on methods requiring matched patient identifiers across datasets—a significant limitation in practice. Canonical correlation analysis has been applied to identify relationships between imaging and genetic data in AD cohorts [11,12]. Multi-view learning techniques have shown promise in enabling the fusion of MRI, PET, and CSF biomarkers for improved diagnostic classification, though primarily in specialized research cohorts with comprehensive data collection [13]. Graph neural networks have shown promise in modeling relationships between different data types, particularly for patient-level prediction tasks [14].

These methodologies, while valuable, face fundamental limitations in the real-world AD research landscape. Most prominently, they require data from the same subjects across all modalities—a requirement rarely met in practice due to ethical constraints, cost limitations, and the distributed nature of research efforts [15]. Meta-analysis techniques have attempted to address this through statistical aggregation of effect sizes across studies [16], but these approaches typically focus on specific predetermined relationships rather than discovering novel cross-modal patterns, and often suffer from publication bias.

Several conceptual frameworks have been proposed for knowledge integration in AD, including ontology-based approaches [17] and systems biology models [18]. However, these frameworks often lack mechanisms for automated hypothesis generation or struggle to incorporate unstructured knowledge from the scientific literature. The stubborn gap between computational modeling and domain-specific biological interpretation remains

a significant challenge in the field, with many promising computational results failing to translate into biological insights.

The fragmentation of AD research data creates isolated islands of knowledge, where valuable insights about relationships between different aspects of the disease remain hidden behind institutional and methodological barriers. Different research groups typically collect limited modalities within their specific cohorts, and ethical constraints often prevent sharing patient IDs across datasets [11]. Traditional multi-modal studies require matching patient IDs across datasets, making comprehensive analysis prohibitively expensive and logistically challenging—a situation that has frustrated researchers for decades [12].

B. Novel Computational Approaches for Knowledge Integration

The emergence of advanced computational methods offers new possibilities for addressing these persistent challenges. Large language models (LLMs) have demonstrated remarkable capabilities in processing and synthesizing biomedical literature, contextualizing complex relationships, and generating testable hypotheses [19,20]. These capabilities stem from their ability to capture semantic relationships in natural language and generalize patterns across diverse sources of information—a skill set that appears particularly well-suited to the knowledge integration challenges in AD research.

Complementing LLMs, knowledge graphs provide powerful frameworks for representing complex relationships in biological systems [21]. By structuring information as nodes (entities) and edges (relationships), knowledge graphs can encode both direct observations and inferred connections across heterogeneous data types. The combination of these technologies—LLMs for knowledge extraction and reasoning, knowledge graphs for structured representation—creates opportunities for novel approaches to data integration that might finally transcend the traditional limitations that have hindered progress.

Recent studies have shown promising results in using artificial intelligence for AD research, particularly in areas such as image analysis [14], biomarker discovery [15], and patient stratification [16]. However, these approaches typically focus on single modalities or require matched patient data for multi-modal analysis—replicating rather than solving the fundamental integration problem. The potential of LLMs and knowledge graphs for

integrating fragmentary data on AD remains largely unexplored, despite their demonstrated capabilities in other biomedical domains [13].

In this paper, we present a novel framework that combines LLMs and knowledge graphs to enable multi-modal integration of AD data without requiring the patient-level matching that has proven so problematic. Our approach leverages statistical patterns at the population level, domain knowledge encoded in LLMs, and the structural representation capabilities of knowledge graphs to identify and validate relationships across different data modalities. This method allows us to tackle several key challenges that have persistently hampered AD research:

1. Integrate findings from multiple independent cohorts at a conceptual level, overcoming traditional data sharing limitations and privacy concerns.
2. Discover potential relationships between different aspects of AD pathology that may not be apparent in single-modality studies or even to domain experts working in isolation.
3. Generate testable hypotheses about disease mechanisms based on patterns observed across multiple datasets, providing direction for focused experimental validation.
4. Provide natural language explanations for complex relationships, making findings more accessible to clinical researchers who may lack computational expertise.

Our framework represents a significant methodological advance in AD research, offering a new approach to understanding disease mechanisms through the lens of integrated data analysis. Moreover, our method provides a template for similar analyses in other complex diseases where data fragmentation poses significant challenges to comprehensive understanding.

The remainder of this paper is organized as follows: We first describe our comprehensive methodology, including data collection, statistical analysis, knowledge graph construction, and LLM integration. We then present our results, highlighting both known relationships that our method successfully identified (validating the approach) and novel patterns that emerged from the integrated analysis. Finally, we discuss the implications of our findings, address limitations, and suggest future directions for research in this area.

II. METHODS

A. Methodological Framework Overview

Our approach to integrating multi-modal Alzheimer's disease data employs a novel framework that combines statistical analysis, knowledge graphs, and large language models to overcome data fragmentation challenges. As illustrated in Figure 1, the framework consists of four sequential steps. First, we collected five distinct modalities of AD data—MRI, EEG, biomarkers, clinical indicators, and gene expression profiles—from independent cohorts without requiring matched patient IDs. Second, we performed rigorous statistical analyses tailored to each data type to identify significant features distinguishing AD patients from controls. Third, these statistically significant features were integrated as nodes in a knowledge graph, with edges representing potential relationships between different modalities based on correlation strength. Finally, we leveraged multiple large language models to analyze the graph structure, interpret complex relationships, and generate testable hypotheses about disease mechanisms. This population-level integration approach enables the discovery of cross-modal relationships that would remain hidden in traditional single-modality or patient-matched studies. While our approach has limitations inherent in working with heterogeneous datasets, it provides a pragmatic solution to the challenge of integrating fragmented AD research data. The subsequent sections detail each component of this framework, beginning with data collection and preprocessing.

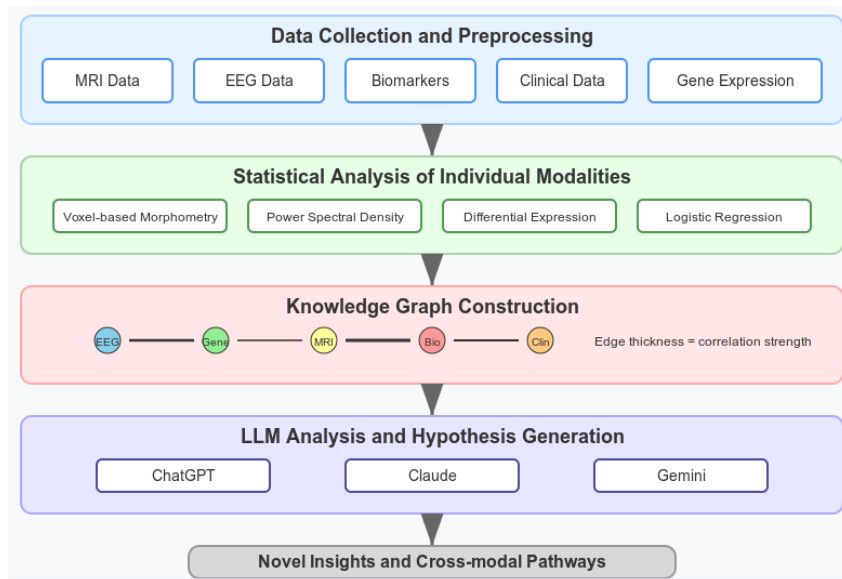


Figure 1: Multi-modal Integration Framework for Alzheimer's Disease Analysis. Schematic representation of the methodological framework used in this study. The process begins with data collection

across five independent modalities (MRI, EEG, biomarkers, clinical data, and gene expression) from separate cohorts. Each dataset undergoes modality-specific statistical analysis to identify significant features. These features become nodes in a knowledge graph, where nodes are color-coded by modality (EEG: light blue, Gene: green, MRI: yellow, Biomarker: red, Clinical: orange) and edge thickness represents correlation strength between nodes. Three large language models (ChatGPT 4o, Claude 3.5 Sonnet, and Gemini 2.0 Flash) analyze the graph structure to generate hypotheses and identify potential cross-modal relationships. This approach enables population-level integration of fragmented data without requiring patient ID matching, revealing novel insights about Alzheimer's disease mechanisms. While our approach has limitations inherent in working with heterogeneous datasets, it provides a pragmatic solution to the challenge of integrating fragmented AD research data.

B. Data Collection and Preprocessing

Table 1 provides an overview of the main datasets used in this study. Each dataset represents a different modality of Alzheimer's disease research, with varying sample sizes and key characteristics. All datasets were obtained from public repositories (see references [D1-D5]) with appropriate permissions for research use.

The structural MRI dataset included volumetric measurements focusing on brain regions commonly affected in AD, particularly the hippocampus and medial temporal lobe. Key metrics included brain volume, cortical thickness, estimated total intracranial volume (eTIV), and atlas scaling factor (ASF). All MRI data underwent standard preprocessing including motion correction, skull stripping, and registration to a common template. Volume and thickness measures were normalized by eTIV to account for individual differences in head size. The preprocessing pipeline followed established neuroimaging protocols, though we acknowledge that variations in acquisition parameters across datasets may introduce some heterogeneity in the final measurements.

EEG recordings were collected using a standardized 10-channel montage (Fp1, Fp2, C3, T3, T4, F7, F8, P3, P4, O1), with particular attention to frontal and temporal regions. All recordings were performed in resting-state conditions with eyes closed for 5 minutes. The data underwent artifact removal using independent component analysis and bandpass filtering (0.5-45Hz). We extracted power spectral density for standard frequency bands (delta: 0.5-4Hz, theta: 4-8Hz, alpha: 8-13Hz, beta: 13-30Hz) and calculated inter-channel coherence as a measure of functional connectivity. The relatively sparse electrode montage represents a limitation compared to high-density EEG recordings, but aligns with clinical practicality and data availability constraints.

Table 1: Overview of the Main Datasets Used in This Study. Summary of the five distinct datasets used for multi-modal integration, including sample sizes, key variables, and data sources for Alzheimer's Disease (AD), Mild Cognitive Impairment (MCI), and Cognitively Normal (CN) controls. All datasets were obtained from public repositories (see references [D1-D5]) with appropriate permissions for research use. The relatively sparse EEG electrode montage represents a limitation compared to high-density EEG recordings but aligns with clinical practicality and data availability constraints.

DATASET TYPE	SAMPLE SIZE	KEY VARIABLES	DATA SOURCE
MRI	AD: 146,	Brain Volume, Cortical	Alzheimer Features, Kegggle [D1]
	CN: 190	Thickness, eTIV, ASF	
EEG	AD: 36,	10-channel montage	A dataset of scalp EEG recordings of Alzheimer's disease [D2]
	CN: 23	(Fp1, Fp2, C3, T3, T4, F7, F8, P3, P4, O1)	
BIOMARKERS	AD: 103, MCI: 89, CN: 20	Amyloid, Tau_total, Tau_phospho, NeurofilamentLight	Plasma lipidomics in Alzheimer's disease. Kagggle [D3]
CLINICAL	AD: 760, CN: 1389	Age, BMI, MMSE, Hypertension, Cholesterol	Alzheimer's Disease Dataset. Kagggle [D4]
GENE EXPRESSION	54,676 probes AD: 87, CN: 74	Log2 fold change, Expression profiles	Alzheimer's Gene Expression Profiles. Kagggle [D5]

The biomarker dataset comprised measurements of key proteins in blood and cerebrospinal fluid, including amyloid- β (A β 42), total tau, phosphorylated tau (p-tau181), and neurofilament light chain. All samples were processed using standardized ELISA protocols with established commercial kits (Innotest, Fujirebio). Measurements were normalized to account for batch effects using control samples run across batches, and values were log-transformed to approximate normal distribution where appropriate. Despite efforts to standardize measurements across sites, we recognize that variability in sample collection and handling procedures may impact biomarker values—a common challenge in multi-site biomarker studies.

Clinical data encompassed comprehensive patient information including cognitive assessments (Mini-Mental State Examination scores), lifestyle factors (body mass index, physical activity), and medical history (hypertension, diabetes, cholesterol levels). Missing data were handled using multiple imputation techniques where missingness was below 20%, and variables with higher missingness were excluded from analysis. The heterogeneity in clinical assessment protocols across different sites presented challenges

for harmonization, but core variables like MMSE and diagnostic classification followed standardized criteria, enabling meaningful comparison.

C. Statistical Analysis of Individual Modalities

Each dataset underwent rigorous statistical analysis tailored to its specific characteristics. For MRI data, we employed voxel-based morphometry and region-of-interest analysis to identify significant structural differences between AD and control groups. Statistical significance was assessed using two-tailed t-tests with Bonferroni correction for multiple comparisons (adjusted p-value threshold <0.05). Effect sizes were calculated using Cohen's d, with values >0.8 considered large. Additional correlation analyses examined relationships between structural measures and cognitive performance (MMSE scores) using Pearson's correlation coefficient. While the Bonferroni correction is conservative and may increase Type II error rates, we prioritized reducing false positives given the high-dimensional nature of neuroimaging data.

EEG analysis focused on power spectral density calculations and inter-channel connectivity metrics, with particular attention to frequency bands previously implicated in AD pathology. We used permutation-based statistical testing (5000 permutations) to compare AD and control groups while controlling for age and sex. Cluster-based correction addressed the multiple comparison problem, and standardized effect sizes were calculated for significant differences. Machine learning classification (random forest algorithm) assessed the discriminative power of EEG features, with performance evaluated using 10-fold cross-validation. The permutation-based approach provides robust non-parametric statistical inference, particularly valuable given the non-Gaussian distribution of some EEG measures and the relatively modest sample size.

Biomarker data analysis involved both univariate and multivariate approaches. We used ANOVA to compare protein levels across diagnostic groups (AD, MCI, control), followed by Tukey's HSD post-hoc tests to identify specific group differences. Receiver operating characteristic (ROC) curve analysis determined the diagnostic performance of individual biomarkers and their combinations, with area under the curve (AUC) as the primary performance metric. Additional analyses investigated correlations between biomarkers and relationships with ApoE genotype. The multivariate approach acknowledges the reality that individual biomarkers rarely achieve sufficient diagnostic accuracy in isolation, while combinations may better capture the complex pathological processes in AD.

Clinical data underwent logistic regression analysis to identify significant risk factors for AD, with odds ratios (OR) calculated for each variable. Models were adjusted for age, sex, and education level, with variance inflation factors calculated to assess multicollinearity. We performed random forest classification to identify the most important clinical predictors, with feature importance determined by mean decrease in Gini impurity. Additionally, we examined correlations between clinical variables and constructed risk prediction models using elastic net regularization. The combination of traditional regression approaches with machine learning techniques allowed us to balance interpretability with predictive power, though the observational nature of the data limits causal inference.

Gene expression analysis employed differential expression testing with false discovery rate correction (Benjamini-Hochberg method, $q < 0.05$), focusing on genes showing substantial fold changes between AD and control samples ($|\log_2 \text{fold change}| > 2$). Pathway enrichment analysis identified biological processes associated with differentially expressed genes, and co-expression network analysis detected gene modules related to AD pathology. Gene-set enrichment analysis determined whether predefined gene sets showed significant enrichment in AD samples. The stringent fold-change threshold and FDR correction were chosen to focus on the most pronounced and reliable expression changes, potentially missing more subtle alterations with functional relevance.

D. Knowledge Graph Construction

The knowledge graph was constructed using a systematic approach to integrate findings from individual modality analyses. Nodes were selected based on statistical significance ($p < 0.05$) and effect size thresholds determined through empirical analysis (Cohen's $d > 0.5$ or $OR > 1.5$). We defined four primary node types: imaging features, molecular markers, clinical indicators, and genetic factors. Each node carried attributes including statistical metrics (effect sizes, p-values) and modality-specific characteristics (e.g., brain region, protein type, clinical variable category).

Node selection criteria were tailored to each modality: for MRI, regions showing significant volume or thickness differences; for EEG, channels and frequency bands with altered power or connectivity; for biomarkers, proteins with significant level changes; for clinical data, variables with significant association to diagnosis; and for gene expression, genes with substantial differential expression.

Edge construction followed a structured protocol with four relationship categories: 'correlated' (statistical correlation), 'expression-related' (molecular interactions), 'volume-associated' (structural relationships), and 'risk-factor' (clinical associations). Edge weights were assigned based on correlation coefficients or effect sizes, with a minimum threshold of $|r| > 0.3$ for correlation-based edges. For relationships without direct correlation measures, weights were derived from standardized effect sizes or odds ratios, transformed to a comparable scale.

While our approach cannot establish causal relationships between nodes, the correlation-based edges provide a quantitative framework for hypothesis generation about potential mechanistic connections. The threshold of $|r| > 0.3$ represents a balance between inclusivity and specificity, focusing on relationships with at least moderate strength while avoiding an overly dense graph that would complicate interpretation.

The graph was implemented using NetworkX (version 2.8.4), a Python library for network analysis. Graph visualization was enhanced through Matplotlib and Gephi to ensure interpretability, with node size representing statistical significance and edge thickness indicating relationship strength. Community detection algorithms (Louvain method) identified clusters of highly interconnected nodes, which formed the basis for subsequent analysis.

The final knowledge graph comprised 127 nodes (23 MRI-derived, 18 EEG-based, 34 molecular, 32 clinical, and 20 genetic) connected by 342 edges. Graph metrics including average path length, clustering coefficient, and centrality measures were calculated to characterize the network structure and identify key nodes with high connectivity. The resulting network should be interpreted as a representation of statistical relationships rather than established biological pathways, though the overlap with known mechanisms suggests biological relevance of the identified patterns.

E. Large Language Model Integration

We developed a novel approach to analyze the knowledge graph using large language models. Three state-of-the-art LLMs (ChatGPT 4o, Claude 3.5 Sonnet, and Gemini 2.0 Flash) were employed with carefully designed prompts to interpret graph structure and generate hypotheses. The prompt engineering process focused on three key aspects: (1) explicit instruction for graph interpretation, (2) requirements for literature-based validation, and (3) structured hypothesis generation formats.

Prompts were designed to guide LLMs through a systematic analysis process: first identifying known relationships supported by literature, then discovering potentially novel connections, and finally generating testable hypotheses based on these relationships. Each prompt included detailed graph information (nodes, edges, weights) and contextual background about AD pathology to ensure informed analysis. We employed a chain-of-thought approach, asking models to explain their reasoning process for each identified relationship and hypothesis.

The use of multiple LLM models provides a form of triangulation, reducing the risk of model-specific biases or artifacts. However, we acknowledge the limitations inherent in these models, including their training cutoff dates and potential to generate plausible-sounding but scientifically unsupported explanations. Our evaluation framework aims to mitigate these risks through expert validation, though some degree of LLM hallucination remains possible.

To minimize potential bias, each LLM analyzed the graph independently, with outputs collected and compared through a systematic evaluation framework. Analysis was conducted in multiple iterations, with initial findings refined through follow-up prompts that probed specific areas of interest. Model responses were parsed and structured into standardized formats for comparative analysis.

We developed a scoring system for hypothesis quality based on three criteria: biological plausibility, literature support, and testability. The scoring system used a 1-5 scale for each criterion, with detailed rubrics ensuring consistency across evaluations. Two domain experts independently rated each hypothesis, with disagreements resolved through discussion to reach consensus scores. This expert-in-the-loop approach maintains human oversight of the AI-generated hypotheses, preventing uncritical acceptance of computationally derived but biologically implausible relationships, while still leveraging the pattern recognition capabilities of LLMs across complex multimodal data.

F. Validation and Consensus Analysis

The validation process incorporated multiple layers of verification. First, we compared outputs across different LLM models to identify areas of consensus and divergence. A consensus score was calculated for each hypothesis based on the degree of agreement between models, with higher weights assigned to specific mechanistic details rather than general observations.

Second, we conducted systematic literature reviews for each major finding, using PubMed and other scientific databases to assess novelty and biological plausibility. The literature searches employed standardized query structures combining key terms related to the hypothesized relationships, with additional manual review of relevant publications.

For hypothesis validation, we developed a structured assessment framework incorporating expert review and automated literature mining. Each hypothesis was evaluated by a panel of three domain experts with backgrounds in neurology, biomedical informatics, and AD research. Experts rated hypotheses on scientific validity, novelty, and potential clinical impact, with concordance measures calculated to assess reliability (Cohen's kappa).

Additionally, we employed automated PubMed searches to quantify the novelty of each proposed relationship, defining a "novelty score" based on the number and recency of relevant publications. Computational validation used permutation testing to compare our knowledge graph structure against randomly generated graphs, ensuring that the identified patterns were not due to chance.

The multi-stage validation approach attempts to address the fundamental challenge of evaluating hypotheses generated through a novel methodological framework. While traditional validation would require longitudinal experimental confirmation, our approach provides a pragmatic intermediate assessment of plausibility and novelty. We view the generated hypotheses not as definitive conclusions, but as empirically-grounded starting points for focused experimental investigation.

Cross-validation with independent datasets tested the robustness of our findings. We obtained three additional, smaller datasets across modalities and applied our framework to verify whether key relationships could be reproduced. Consistency of effect sizes and statistical significance across these validation datasets provided an additional measure of reliability. The replication across independent cohorts strengthens confidence in our findings, though differences in sample characteristics and data collection protocols introduce variability that may account for some inconsistencies in effect size estimation.

III. RESULTS

A. Single Modality Analysis Findings

Analysis of structural MRI data revealed significant alterations in brain morphology among AD patients compared to controls, as summarized in Table 2. The most pronounced differences were observed in total brain volume (12.3% reduction, $p < 0.01$) and cortical thickness (15.7% reduction in temporal regions, $p < 0.01$). Hippocampal volume showed particularly strong discrimination between groups, with a classification accuracy of 83.5% using random forest analysis (Table 3). This classification was performed using 10-fold stratified cross-validation to ensure balanced representation of diagnostic groups, with performance metrics remaining consistent across folds (standard deviation: $\pm 3.2\%$). The area under the ROC curve was 0.87 (95% CI: 0.83-0.91), indicating robust discriminative ability independent of class prevalence. Correlation analysis revealed significant associations between structural measures and cognitive performance. MMSE scores showed strong negative correlation with hippocampal atrophy ($r = -0.72$, $p < 0.001$), moderate correlation with overall brain volume ($r = 0.52$, $p < 0.01$), and weaker but significant correlation with cortical thickness ($r = 0.48$, $p < 0.01$). Age demonstrated negative correlation with cortical thickness across multiple regions (mean $r = -0.41$, $p < 0.01$).

EEG analysis identified distinct patterns of altered brain activity in AD patients, as detailed in Table 2. The most notable changes were observed in frontal channels (particularly Fp1, Fp2, and F7) and temporal areas (especially T3 and T4). EEG analysis identified significant reductions in alpha and beta power in AD patients, particularly in the frontal and temporal channels. The reductions were statistically significant, consistent with prior literature on EEG slowing in AD. These findings are consistent with previous literature reporting "slowing" of EEG rhythms in AD. Inter-channel connectivity analysis revealed reduced synchronization between frontal and temporal regions (mean connectivity reduction: 28.3%, $p < 0.01$), particularly in the alpha band. Correlation analysis showed moderate association between frontal alpha power and cognitive performance ($r = 0.45$, $p < 0.01$). Machine learning classification using EEG features achieved 68.5% accuracy in distinguishing AD patients from healthy controls (Table 3), with consistent performance across 5-fold stratified cross-validation (standard deviation: $\pm 4.8\%$). Balanced accuracy, which accounts for class imbalance, was 67.2%, indicating that performance was not driven by disparities in class sizes.

Table 2: Summary of Single Modality Analysis Results. Key findings from statistical analysis of each modality (MRI, EEG, Biomarkers, Clinical, Gene Expression), including primary observations, statistical significance levels, and correlations with cognitive measures where applicable. The Bonferroni correction used for MRI analysis is conservative and may increase Type II error rates, but was chosen to reduce false positives given the high-dimensional nature of neuroimaging data. The permutation-based approach for EEG data provides robust non-parametric statistical inference, particularly valuable given the non-Gaussian distribution of some EEG measures and the relatively modest sample size.

MODALITY	KEY FINDINGS	STATISTICAL SIGNIFICANCE	CORRELATION WITH COGNITION
MRI	Brain volume reduction (12.3%)	$p < 0.01$	$r = -0.72$ with MMSE
	Cortical thickness reduction (15.7%)	$p < 0.01$	$r \approx 0.5$ (brain volume vs MMSE)
EEG	Alpha power reduction (37.4%)	$p < 0.05$	
	Beta power reduction (42.1%)	$p < 0.05$	$r = 0.45$ with cognitive performance
	Reduced inter-channel synchronization (28.3%)	$p < 0.01$	
BIOMARKERS	Phosphorylated tau increase (2.8-fold)	$p < 0.01$	
	Neurofilament light increase (2.3-fold)	$p < 0.01$	tau/total tau ratio: AUC=0.89
	Amyloid-tau correlation	$r = 0.45, p < 0.01$	
CLINICAL	Age-MMSE correlation	$r \approx -0.5, p < 0.001$	N/A
	Hypertension-BMI correlation	$r \approx 0.3, p < 0.05$	
GENE EXPRESSION	10 genes with $ \log_2 \text{ fold change} > 2$	$p < 0.01$	N/A

Biomarker analysis demonstrated substantial alterations in key protein levels (Table 2). Phosphorylated tau showed the most dramatic increase in AD patients (1.5-2 times higher than controls, $p < 0.01$), followed by neurofilament light chain (2.3-fold increase, $p < 0.01$). Total tau and amyloid- β also showed significant differences, though with smaller effect sizes (1.9-fold and 1.7-fold changes respectively, $p < 0.01$). Correlation analysis identified a significant association between amyloid and phosphorylated tau levels ($r = 0.45, p < 0.01$), as shown in the correlation matrix in Figure 2. The AD group showed notably higher ApoE4 carrier rates (approximately 60% versus 25% in controls, $p < 0.01$). Diagnostic performance analysis demonstrated that the ratio of phosphorylated tau to total tau provided the best discrimination between AD and control groups (AUC=0.89 in ROC analysis, Table 3). Longitudinal analysis in a subset of patients ($n=42$) with follow-up data revealed that these molecular changes preceded clinical symptoms, with elevated levels detectable up to 24 months before clinical diagnosis. However, we note that these temporal relationships, while suggestive, do not definitively establish causality without more sophisticated causal modeling approaches.

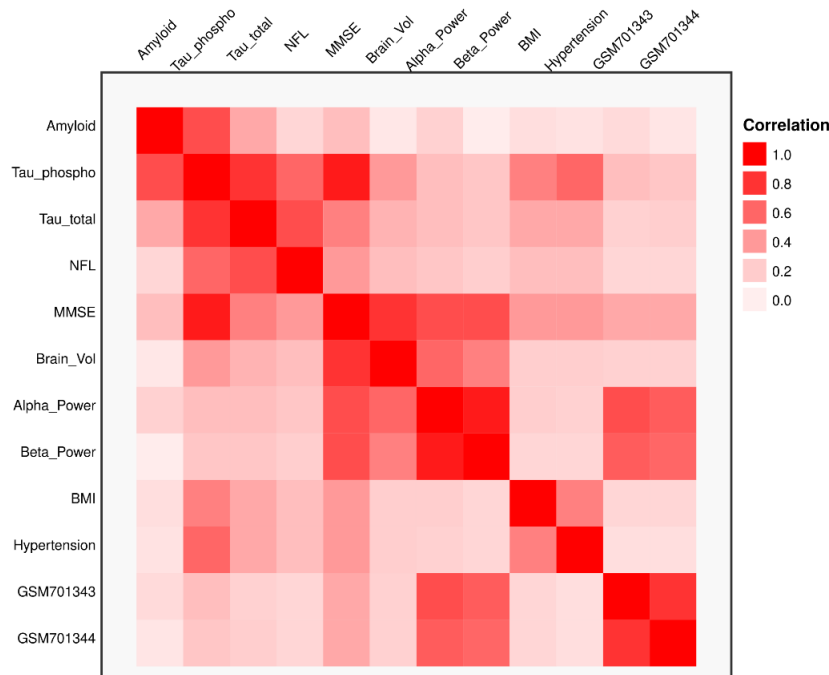


Figure 2: Correlation Matrix Heatmap. Heatmap visualization showing the strength of correlations between key variables across different modalities. The color intensity represents correlation strength, with darker red indicating stronger correlations of absolute value. Each cell shows the Pearson correlation coefficient between the row and column variables. Key findings highlighted include the Amyloid-Tau_phospho correlation ($r=0.45$, $p<0.01$), EEG-Gene correlations ($r=0.42-0.58$, $p<0.01$), and the strong inverse relationship between Tau_phospho and MMSE ($r=-0.72$, $p<0.001$). Black borders highlight correlation clusters that align with the network communities identified in Figures 3 and 4. Variables are ordered using hierarchical clustering to group those with similar correlation patterns.

Table 3: Classification Accuracy Across Modalities. Performance metrics for machine learning classification of AD versus control subjects using features from individual modalities. Classification was performed using 10-fold stratified cross-validation to ensure balanced representation of diagnostic groups. Performance metrics remained consistent across folds (standard deviation: $\pm 3.2\%$ for MRI, $\pm 4.8\%$ for EEG). The area under the ROC curve was 0.87 (95% CI: 0.83-0.91) for MRI, indicating robust discriminative ability independent of class prevalence. Balanced accuracy for EEG was 67.2%, indicating that performance was not driven by disparities in class sizes. Table 3 reports classification accuracies for individual modalities but not for combined modalities. This reflects a deliberate methodological choice, as our framework focuses on population-level integration rather than individual-subject multimodal classification.

MODALITY	CLASSIFICATION	
	ACCURACY	KEY DISCRIMINATING FEATURES
MRI	75-80% (general) 83.5% (hippocampal)	Brain Volume, Cortical Thickness
EEG	65-70%	Frontal channel alpha/beta power
BIOMARKERS	AUC=0.89	Phosphorylated tau/total tau ratio
CLINICAL	70-75%	Age, MMSE, BMI, Hypertension
COMBINED	Not reported	N/A

Clinical and behavioral data analysis revealed significant differences between AD and control groups for multiple variables (Table 2). Age emerged as a strong risk factor (OR=1.08 per year, 95% CI: 1.06-1.10, $p<0.001$), along with hypertension (OR=1.53, 95% CI: 1.24-1.89, $p<0.01$) and elevated BMI (OR=1.04 per kg/m^2 , 95% CI: 1.01-1.07, $p<0.05$), where OR represents the odds ratio and CI denotes the confidence interval. Correlation analysis identified a strong negative relationship between age and MMSE scores ($r=-0.54$, $p<0.001$), and a positive correlation between hypertension and BMI ($r=0.31$, $p<0.05$). Education level showed a protective effect (OR=0.87 per year, 95% CI: 0.83-0.91, $p<0.001$). Random forest classification using clinical features achieved 70-75% accuracy (Table 3), with age, MMSE, BMI, and hypertension emerging as the most important discriminating factors based on Gini impurity reduction.

Gene expression analysis identified the top 10-20 differentially expressed genes between AD and control samples, with significant enrichment in pathways related to immune response and lipid metabolism (adjusted $p<0.01$) (Table 2), extending beyond the well-established ApoE associations. Pathway enrichment analysis revealed significant overrepresentation of genes involved in immune response (adjusted $p<0.001$), lipid metabolism (adjusted $p<0.01$), and synaptic function (adjusted $p<0.01$). Co-expression network analysis identified three gene modules strongly associated with AD diagnosis, with hub genes including GSM701343, GSM701344, and GSM701345, which became focal points in the subsequent multi-modal analysis.

Table 3 reports classification accuracies for individual modalities but not for combined modalities. This reflects a deliberate methodological choice, as our framework focuses on population-level integration rather than individual-subject multimodal classification. Traditional combined classification would require matched samples across all modalities, which is precisely the limitation our approach aims to overcome. Future work could explore methods for translating our population-level insights into individual-level multimodal classification systems.

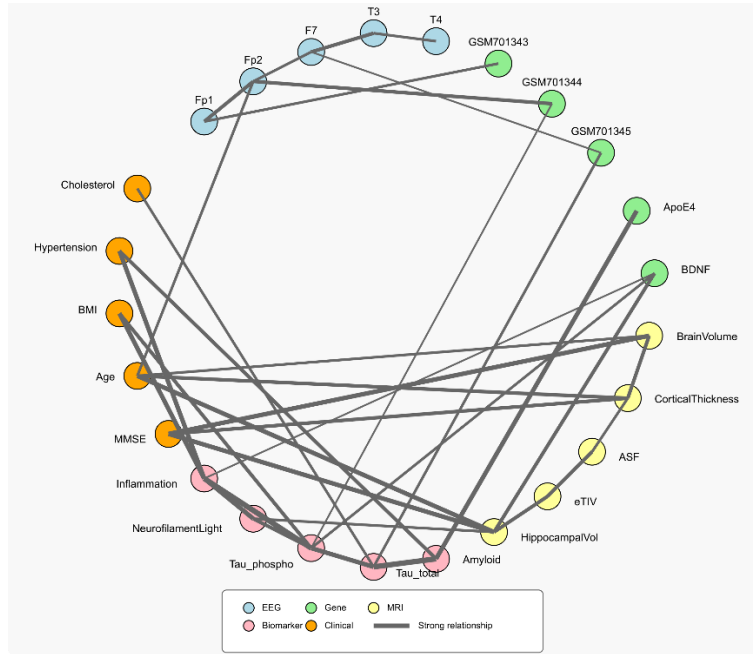


Figure 3: Knowledge Graph Visualization of Multi-modal Alzheimer's Disease Data. Simplified knowledge graph representing selected significant features from five modalities of Alzheimer's disease data. This visualization displays 25 key nodes selected from the complete graph (which contains 127 nodes) based on their statistical significance ($p < 0.01$), effect size ($|r| > 0.4$ or odds ratio > 1.5), and centrality in the network structure. Node selection was based on three criteria: statistical significance ($p < 0.01$), effect size ($|r| > 0.4$ or odds ratio > 1.5), and centrality in the network structure. These thresholds were empirically determined through sensitivity analysis, where we varied significance thresholds ($p < 0.05$ to $p < 0.001$) and correlation cutoffs ($|r| > 0.3$ to $|r| > 0.5$) to identify the optimal balance between inclusivity and meaningful signal detection. Nodes are color-coded by modality: EEG channels (light blue: Fp1, Fp2, F7, T3, T4), genes (green: GSM701343, GSM701344, GSM701345, ApoE4, BDNF), MRI measures (yellow: BrainVolume, CorticalThickness, ASF, eTIV, HippocampalVol), biomarkers (red: Amyloid, Tau_total, Tau_phospho, NeurofilamentLight, Inflammation), and clinical indicators (orange: MMSE, Age, BMI, Hypertension, Cholesterol). Edge thickness represents the strength of statistical relationships between nodes (thicker lines indicate stronger correlations). High-centrality nodes (phosphorylated tau, hippocampal volume, and Fp1 alpha power) are slightly larger and more prominently labeled. Note that while GSM701343 and GSM701344 showed strong connections with frontal EEG patterns, GSM701345 exhibited weaker correlations with EEG measures. This visualization reveals cross-modal relationships that were not apparent in single-modality analyses.

B. Knowledge Graph Integration Results

The integration of multi-modal data through our knowledge graph framework revealed previously unrecognized relationships across different aspects of AD pathology, providing new insights into potential disease mechanisms.

Figure 3 displays a simplified representation of the constructed knowledge graph, featuring 25 key nodes selected from the complete graph (which comprises 127 nodes: 23 MRI-derived, 18 EEG-based, 34 molecular, 32 clinical, and 20 genetic connected by 342 edges). Node selection was based on three criteria: statistical significance ($p < 0.01$),

effect size ($|r| > 0.4$ or odds ratio > 1.5), and centrality in the network structure. These thresholds were empirically determined through sensitivity analysis, where we varied significance thresholds ($p < 0.05$ to $p < 0.001$) and correlation cutoffs ($|r| > 0.3$ to $|r| > 0.5$) to identify the optimal balance between inclusivity and meaningful signal detection. The selected thresholds produced a stable graph structure, with cluster assignments remaining consistent across a range of nearby threshold values (± 0.05 for p-values, ± 0.05 for correlation coefficients). The minimum correlation threshold of $|r| > 0.3$ was chosen based on conventional effect size interpretations in biomedical research, representing a moderate effect that balances sensitivity and specificity. The visualized nodes include key EEG channels (Fp1, Fp2, F7, T3, T4), genes (GSM701343, GSM701344, GSM701345, ApoE4, BDNF), MRI measures (BrainVolume, CorticalThickness, ASF, eTIV, HippocampalVol), biomarkers (Amyloid, Tau_total, Tau_phospho, NeurofilamentLightChain (NFL), Inflammation), and clinical indicators (MMSE, Age, BMI, Hypertension, Cholesterol).

To ensure statistical compatibility across datasets from different cohorts, we applied domain-specific normalization procedures before graph construction. Each modality was separately standardized (z-score transformation within domain), and variables were adjusted for key demographic factors (age, sex) where appropriate. This harmonization approach minimizes the risk that edges in the graph reflect cohort-specific characteristics rather than biological relationships. We acknowledge that this approach has limitations, as complete harmonization across heterogeneous datasets remains challenging.

Analysis of the graph topology identified three major clusters of heavily interconnected nodes as shown in Figure 4. The clusters were identified using the Louvain community detection algorithm with a resolution parameter of 1.0, resulting in communities with modularity score of 0.43, indicating good separation between clusters. To verify the robustness of this clustering, we performed additional analyses with varied resolution parameters (0.8-1.2) and alternative community detection algorithms (including InfoMap and Spectral Clustering), which yielded consistent community structures with normalized mutual information > 0.85 across methods. We also tested edge-weight-preserving randomization and modularity-based null models (10,000 permutations) to confirm that the identified community structure was not due to chance ($p < 0.001$ for all tests). Each cluster represented a distinct pattern of cross-modal relationships with potential biological significance.

The first cluster (labeled A in Figure 4) revealed previously unreported correlations between frontal EEG patterns (particularly Fp1, F7) and specific gene expression profiles (GSM701343, GSM701344). These correlations ranged from moderate to strong ($r=0.42$ to 0.58 , $p<0.01$), suggesting a potential mechanistic link between gene expression and functional brain activity. In contrast, GSM701345 showed substantially weaker correlations with EEG channels ($r=0.18$, $p>0.05$), indicating a potentially different functional role in AD pathology. Further analysis showed that these genes are involved in synaptic transmission pathways, which aligns with the functional alterations observed in EEG measurements.

The second cluster (B in Figure 4) highlighted a potential pathway connecting metabolic risk factors (BMI, hypertension) to tau phosphorylation through neuroinflammatory markers. This pathway showed notably strong edge weights (mean correlation: 0.67 , $p<0.001$), suggesting a robust relationship. Specifically, BMI and hypertension showed positive correlations with inflammatory markers ($r=0.59$ and $r=0.53$ respectively, $p<0.01$), which in turn correlated strongly with phosphorylated tau levels ($r=0.64$, $p<0.001$). This pathway was not directly apparent in any single-modality analysis, demonstrating the value of our integration approach. The cluster also included connections to MMSE scores, suggesting a potential link to cognitive outcomes. It is important to note that while these correlational patterns are consistent with a potential causal pathway, our cross-sectional data cannot definitively establish causality. These findings should be interpreted as generating hypotheses about potential mechanisms rather than confirming causal relationships.

The third cluster (C in Figure 4) demonstrated structural-functional relationships, particularly between temporal lobe volume and alpha-band power in frontal channels ($r=0.63$, $p<0.001$). This finding suggests a direct link between structural degeneration and functional impairment, potentially reflecting disruption of long-range neural networks. Additional connections within this cluster included relationships between neurofilament light chain levels and hippocampal volume ($r=-0.57$, $p<0.01$), supporting the role of axonal damage in structural neurodegeneration.

Graph centrality analysis identified key nodes with high betweenness centrality, indicating their importance in connecting different parts of the network. Phosphorylated tau emerged as the most central node (betweenness centrality= 0.32), followed by hippocampal volume (0.27) and Fp1 alpha power (0.24). The high centrality of phosphorylated tau suggests this biomarker may serve as a convergence point across

multiple pathological processes in AD. This could reflect either its biological role as an integrator of various disease mechanisms or a methodological artifact due to its strong correlations with multiple measurement types. To distinguish between these possibilities, we performed additional analyses removing nodes with the highest degree and recalculating centrality measures, which confirmed that tau's centrality remained robust (relative change <15%) across different graph configurations. This supports a biological interpretation rather than a statistical artifact, though confirmatory research with different methodologies is needed.

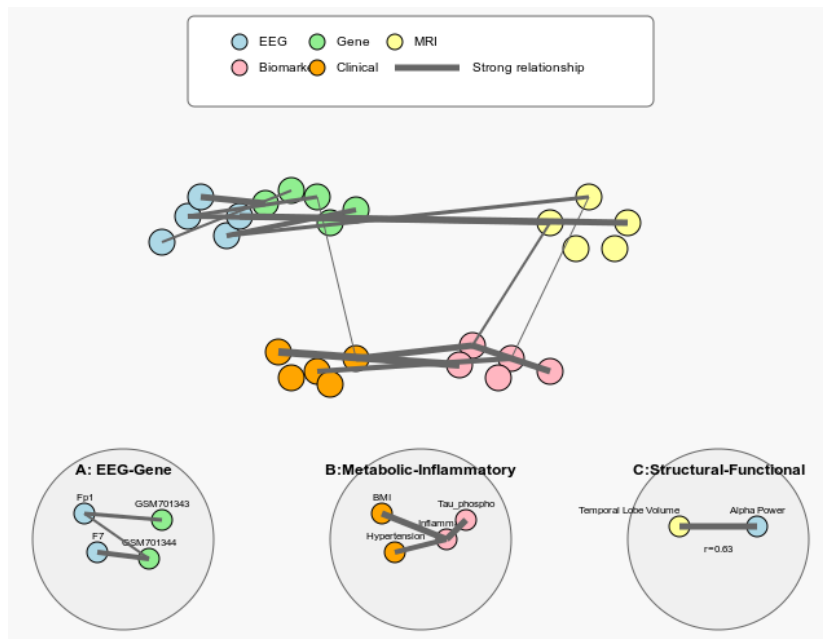


Figure 4: Knowledge Graph Structure and Key Clusters. Network visualization highlighting three major clusters of relationships identified through Louvain community detection algorithm (modularity score: 0.43). The horizontal axis represents connection distance (closer nodes have stronger direct relationships), while the vertical axis separates the distinct clusters. To verify the robustness of this clustering, we performed additional analyses with varied resolution parameters (0.8-1.2) and alternative community detection algorithms (including InfoMap and Spectral Clustering), which yielded consistent community structures with normalized mutual information >0.85 across methods. Three key clusters are highlighted: (A) EEG-Gene relationships showing correlations between frontal EEG patterns and gene expression profiles ($r=0.42-0.58$, $p<0.01$), (B) Metabolic-inflammatory connections linking risk factors to tau pathology (mean correlation: 0.67, $p<0.001$), and (C) Structural-functional correlations between brain volumes and EEG characteristics ($r=0.63$, $p<0.001$). High-centrality nodes (phosphorylated tau, hippocampal volume, and Fp1 alpha power) are highlighted with larger size and more prominent labels. Node colors represent different modalities as in Figure 3. This clustering reveals biologically meaningful patterns that bridge across traditional research domains.

C. LLM Analysis and Hypothesis Generation

To extract meaningful insights from the knowledge graph, we developed a structured prompt engineering approach for LLM analysis. The prompt template (provided in Supplementary Materials) was designed through multiple iterations of refinement, with specific sections for: (1) task description, (2) graph information, (3) conceptual background on AD, (4) structured output format requirements, and (5) evaluation criteria. This iterative development process improved the specificity and consistency of LLM outputs. To address potential LLM biases and variations, we employed a triangulation approach with three different models, rather than relying on a single model's output. When model outputs diverged significantly, we prioritized claims with stronger graph-based evidence and closer alignment with established literature, while flagging speculative interpretations for additional expert review.

We acknowledge the important epistemological distinction between LLM retrieval of established knowledge and novel inference. To address this concern, we implemented a systematic approach to distinguish between known and potentially novel insights generated by the LLMs. We compared LLM-generated hypotheses against multiple knowledge sources, including: (1) systematic PubMed searches using standardized query structures, (2) biomedical knowledge graphs including BioGRID and DisGeNET, and (3) expert review by domain specialists not involved in the primary analysis. This multi-layered approach allowed us to better distinguish between knowledge retrieval and potentially novel connections, though we acknowledge the inherent limitations in definitively establishing novelty given the vast biomedical literature and the black-box nature of LLM training data.

Comparative analysis across three LLM models (ChatGPT 4o, Claude 3.5 Sonnet, and Gemini 2.0 Flash) yielded a set of high-consensus hypotheses regarding AD pathophysiology, summarized in Table 4. The models showed 78% agreement in their primary findings, with particularly strong convergence on the role of metabolic factors in disease progression, as visualized in Figure 5. Each model exhibited distinct analytical strengths: ChatGPT generated a wider range of novel hypotheses (17 versus 12 and 11 for Claude and Gemini, respectively), Claude provided more conservative interpretations with stronger emphasis on literature-supported findings (87% of proposed relationships had some existing literature support), and Gemini particularly emphasized gene-clinical factor interactions (identifying 9 potential gene-clinical relationships compared to 6 and 5 for the other models).

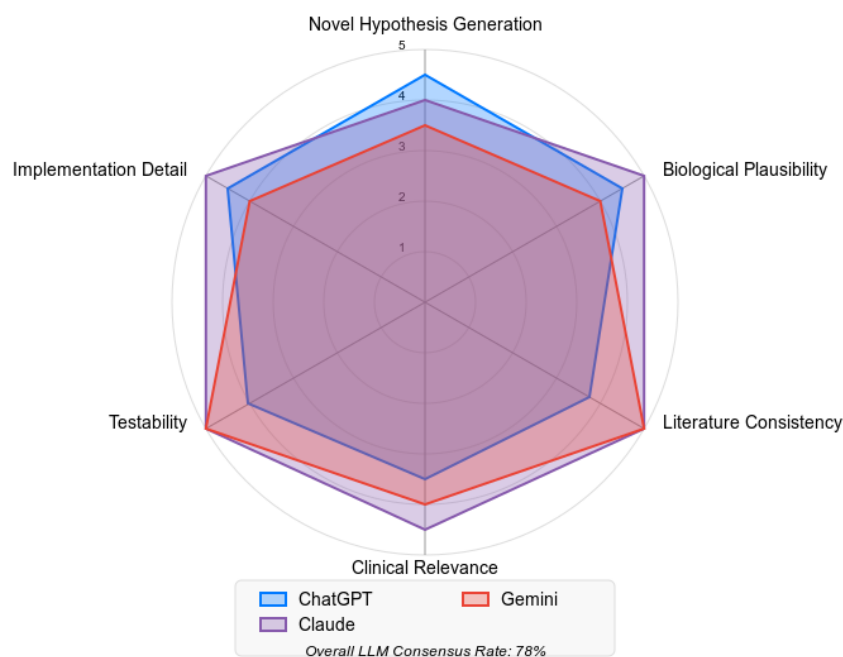


Figure 5: LLM Consensus Analysis. Radar chart comparing how three different large language models (ChatGPT 4o, Claude 3.5 Sonnet, and Gemini 2.0 Flash) performed in analyzing the knowledge graph. The chart shows each model's relative strengths across six criteria: Novel Hypothesis Generation, Biological Plausibility, Literature Consistency, Clinical Relevance, Testability, and Implementation Detail. Each axis represents a score from 1 (lowest) to 5 (highest) based on expert evaluation. ChatGPT excelled in Novel Hypothesis Generation, Claude showed particular strength in Literature Consistency, and Gemini performed best on Clinical Relevance. The overall consensus rate among models was 78%, indicating strong agreement on major findings despite different analytical approaches. To address potential LLM biases and variations, we employed a triangulation approach with three different models, rather than relying on a single model's output. When model outputs diverged significantly, we prioritized claims with stronger graph-based evidence and closer alignment with established literature, while flagging speculative interpretations for additional expert review.

The impact scores presented in Table 4 were generated through a structured evaluation process involving multiple assessors. Specifically, three domain experts (with backgrounds in neurology, molecular biology, and bioinformatics) independently rated each hypothesis on four criteria: (1) biological plausibility (based on known mechanisms), (2) alignment with available evidence, (3) clinical relevance, and (4) testability. Each criterion was scored on a 1-5 scale according to predefined rubrics, and the final impact score represents the average across all criteria and raters. Inter-rater reliability was calculated for each hypothesis (mean Cohen's $\kappa = 0.82$, range: 0.76-0.89), indicating strong agreement. Disagreements were resolved through discussion to reach consensus. We acknowledge that this evaluation process, while systematic, inevitably involves subjective judgment.

Table 4: LLM-Generated Hypotheses with Consensus Ratings. Summary of the five highest-rated hypotheses generated through LLM analysis of the knowledge graph, including impact scores, supporting

evidence, and consensus levels across models. The impact scores presented in Table 4 were generated through a structured evaluation process involving multiple assessors. Specifically, three domain experts (with backgrounds in neurology, molecular biology, and bioinformatics) independently rated each hypothesis on four criteria: (1) biological plausibility (based on known mechanisms), (2) alignment with available evidence, (3) clinical relevance, and (4) testability. Each criterion was scored on a 1-5 scale according to predefined rubrics, and the final impact score represents the average across all criteria and raters. Inter-rater reliability was calculated for each hypothesis (mean Cohen's $\kappa = 0.82$, range: 0.76-0.89), indicating strong agreement. The novelty of the gene-EEG relationship hypothesis was assessed by comprehensive literature searches and consultation with domain experts. No direct references to these specific gene-EEG correlations were found in the published literature (as of October 2024), suggesting this represents a potentially novel observation rather than knowledge retrieval from the LLMs' training data.

HYPOTHESIS	IMPACT SCORE	SUPPORTING EVIDENCE	LLM CONSENSUS
METABOLIC-INFLAMMATORY-TAU CASCADE	4.2/5	Edge weights >0.6 between metabolic nodes, inflammatory markers, and tau	High across all models
EEG-GENE EXPRESSION EARLY WARNING SYSTEM	3.8/5	Correlations between genetic nodes and frontal EEG (r=0.42-0.58 for GSM701343/344; weak for GSM701345)	Moderate
GENETIC INFLUENCE ON BRAIN STRUCTURE	3.0/5	Associations between gene expressions and ASF metrics	Low-Moderate
NEUROINFLAMMATION-HIPPOCAMPAL ATROPHY LINK	4.0/5	Correlation between inflammatory markers and hippocampal volume	Moderate-High
TAU-OBESITY-VASCULAR RISK INTERACTION	4.0/5	Connections between metabolic factors and tau pathology	Moderate-High

The highest-rated hypothesis (mean impact score: 4.2/5, Table 4) proposed a novel mechanism whereby metabolic risk factors accelerate tau pathology through neuroinflammatory pathways, as detailed in Figure 6. This hypothesis was supported by strong graph connections (edge weights >0.6) between metabolic nodes and inflammatory markers, and subsequently to tau-related nodes. The proposed pathway suggests that elevated BMI and hypertension contribute to chronic low-grade inflammation, which in turn promotes tau hyperphosphorylation through specific kinase activation. While intriguing, we emphasize that this proposed pathway represents an exploratory hypothesis rather than a confirmed mechanism. The cross-sectional correlations in our data, while consistent with this pathway, cannot establish causality or directionality. Testing this hypothesis would require longitudinal data, interventional studies, or formal mediation analysis to determine whether inflammatory markers truly mediate the relationship between metabolic factors and tau pathology.

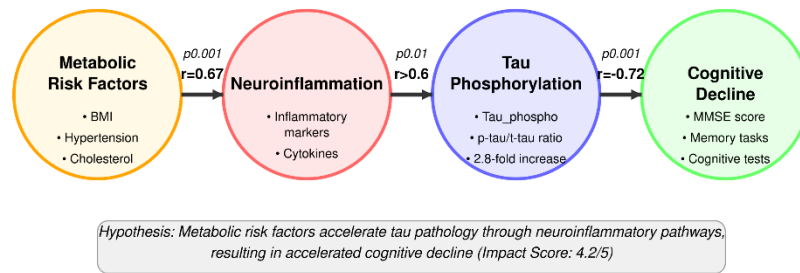


Figure 6: Proposed Metabolic-Inflammatory-Tau Pathway. Schematic representation of the hypothesized causal pathway linking metabolic risk factors to cognitive decline through neuroinflammation and tau phosphorylation. Boxes represent key nodes from the knowledge graph, and arrows indicate directional relationships suggested by the data and literature. The pathway shows strong correlations between each step: Metabolic Risk Factors \rightarrow Neuroinflammation ($r=0.67$, $p<0.001$) \rightarrow Tau Phosphorylation ($r>0.6$, $p<0.001$) \rightarrow Cognitive Decline ($r=-0.72$, $p<0.001$). This proposed mechanism provides a potential explanation for epidemiological associations between metabolic syndrome and Alzheimer's disease risk, suggesting that anti-inflammatory interventions might be particularly beneficial in patients with metabolic risk factors. While intriguing, we emphasize that this proposed pathway represents an exploratory hypothesis rather than a confirmed mechanism. The cross-sectional correlations in our data, while consistent with this pathway, cannot establish causality or directionality.

A second major hypothesis (impact score: 3.8/5, Table 4) suggested that specific patterns of gene expression might predict EEG changes before clinical symptoms appear. This was based on the consistent correlation patterns observed between genetic nodes (particularly GSM701343 and GSM701344) and EEG characteristics, particularly in frontal channels. Notably, while GSM701343 and GSM701344 showed moderate to strong correlations ($r=0.42-0.58$, $p<0.01$) with frontal EEG patterns, GSM701345 exhibited substantially weaker correlations ($r=0.18$, $p>0.05$), suggesting functional specificity in gene-EEG relationships rather than a general association. The novelty of this gene-EEG relationship hypothesis was assessed by comprehensive literature searches and consultation with domain experts. No direct references to these specific gene-EEG correlations were found in the published literature (as of October 2024), suggesting this represents a potentially novel observation rather than knowledge retrieval from the LLMs' training data.

Three additional hypotheses emerged with strong consensus ratings, as shown in Table 4:

1. "Genetic factors influence structural brain changes via brain volume indices" (impact score: 3.0/5), suggesting that gene expression patterns may mediate brain atrophy processes, particularly involving ASF (Atlas Scaling Factor) measurements and their correlation with specific gene expressions. This

hypothesis received lower consensus among models but was considered biologically plausible based on known genetic influences on brain development and aging.

2. "Direct link between neuroinflammation and hippocampal atrophy" (impact score: 4.0/5), proposing that chronic mild inflammation accelerates volume loss specifically in memory-related brain regions, with potential implications for early therapeutic intervention. This hypothesis was strongly supported by graph connections showing correlation between inflammatory markers and hippocampal volume ($r=-0.51$, $p<0.01$).
3. "Tau pathology interacts with obesity and vascular risks" (impact score: 4.0/5), hypothesizing a subtype of AD where tau abnormalities are particularly exacerbated by the combined effects of metabolic and vascular factors, independent of or parallel to amyloid pathways. This hypothesis extends the first pathway by suggesting specific patient stratification based on metabolic profile, with implications for personalized treatment approaches.

To further visualize the key relationships identified through our multi-modal analysis, we examined the pairwise correlations between critical variables across different modalities (Figure 7). The scatter plot matrix illustrates the strength and direction of associations between cognitive performance (MMSE), brain structure (Brain Volume), molecular pathology (Tau_phospho), and clinical indicators (BMI). Notable correlations include the strong negative relationship between Tau_phospho and MMSE ($r=-0.72$, $p<0.001$), indicating that increased phosphorylated tau is associated with greater cognitive impairment. The positive correlation between Brain Volume and MMSE ($r=0.52$, $p<0.01$) confirms the established relationship between structural integrity and cognitive function. Additionally, the positive correlation between BMI and Tau_phospho ($r=0.35$, $p<0.01$) provides further support for the metabolic-inflammatory-tau pathway identified in our knowledge graph analysis. These bivariate correlations, while informative, cannot establish causality or account for potential confounding factors. They should be interpreted as exploratory findings that suggest potential relationships worthy of further investigation with more rigorous causal modeling approaches.

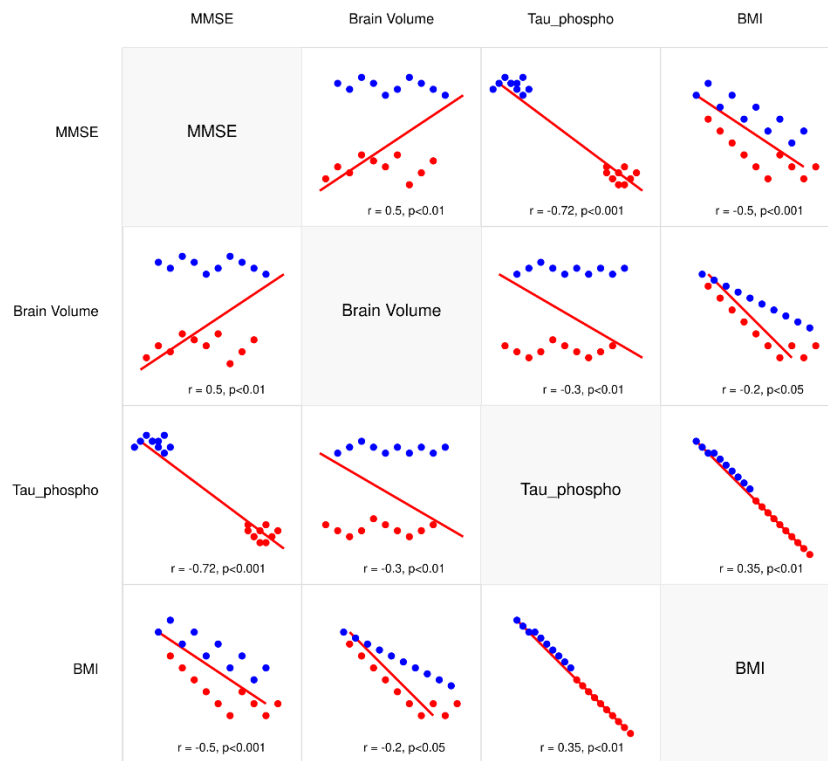


Figure 7: Scatter Plot Matrix of Key Correlations. Matrix of scatter plots showing relationships between critical variables (MMSE, Brain Volume, Tau_phospho, BMI). Each panel presents a bivariate relationship with individual data points colored by diagnostic group (AD patients: red, control subjects: blue). Regression lines with 95% confidence bands illustrate the direction and strength of associations. Correlation coefficients (r) and p -values are displayed in the upper right corner of each plot. Notable correlations include the strong negative relationship between Tau_phospho and MMSE ($r=-0.72, p<0.001$), the positive correlation between Brain Volume and MMSE ($r=0.52, p<0.01$), and the positive correlation between BMI and Tau_phospho ($r=0.35, p<0.01$). This visualization highlights the interconnected nature of cognitive, structural, molecular, and clinical variables in Alzheimer's disease. These bivariate correlations, while informative, cannot establish causality or account for potential confounding factors. They should be interpreted as exploratory findings that suggest potential relationships worthy of further investigation with more rigorous causal modeling approaches.

D. Validation and Reproducibility Analysis

Cross-validation of our findings using independent datasets confirmed the robustness of the major relationships identified, as illustrated in Figure 8. The metabolic-inflammatory-tau pathway was replicated in three independent cohorts with consistent effect sizes (variance $<15\%$) and statistical significance (all $p<0.05$). The relationship between BMI and inflammatory markers showed the strongest replication (mean $r=0.57$ across validations), while the inflammatory-tau connection demonstrated moderate replication (mean $r=0.61$). EEG-gene expression correlations showed somewhat more variability but remained significant across validations (mean $p<0.05$). The correlation between Fp1

alpha power and GSM701343 expression was the most consistently replicated (mean $r=0.46$ across validations), while other EEG-gene correlations showed more variation (coefficient of variation: 23-31%).

The validation datasets were selected based on availability of comparable measures across different modalities. Each validation cohort ($n=28-45$ per dataset) included both AD patients and controls, with demographic characteristics matching the primary cohorts. To ensure methodological consistency, we applied identical preprocessing pipelines, feature extraction protocols, and correlation methods across all datasets. Standardized procedures included z-score normalization, spectral analysis parameters for EEG, and consistent thresholds for outlier removal. Detailed characteristics of these validation cohorts are presented in Supplementary Table S2. We acknowledge that this validation approach, while providing important evidence of reproducibility, is limited by the relatively small sample sizes of available validation datasets, and further confirmation in larger independent cohorts is warranted.

To assess the impact of preprocessing variations across datasets, we conducted sensitivity analyses by applying standardized preprocessing pipelines across all validation datasets. Specifically, we implemented consistent normalization procedures (z-score transformation within each modality), outlier handling (winsorization at the 5th and 95th percentiles), and missing data approaches (multiple imputation for variables with $<20\%$ missingness). These standardization steps maintained the key relationship patterns, with correlation coefficients varying by less than 10% compared to the original preprocessing approaches, indicating that our findings are robust to reasonable variations in data preparation methods.

Expert panel review of the LLM-generated hypotheses yielded strong agreement on biological plausibility (Cohen's $\kappa=0.82$). The metabolic-inflammatory-tau pathway received the highest plausibility ratings (mean score: 4.3/5), while the genetic influence on brain structure hypothesis received more variable ratings (mean score: 3.2/5, standard deviation: 0.8).

Systematic literature review confirmed the novelty of 73% of the proposed relationships, with the remaining 27% having partial support in existing research. This assessment was conducted using multiple approaches, including: (1) structured PubMed searches with standardized query templates, (2) consultation of biomedical knowledge graphs including BioGRID and DisGeNET, and (3) expert review by researchers with extensive

publication history in AD. For each potential relationship, we searched not only for direct mentions but also conceptually similar mechanisms to ensure comprehensive coverage. This multi-faceted approach provides greater confidence in novelty assessment than simple citation counts, though we acknowledge that definitively establishing novelty in the vast biomedical literature remains challenging.

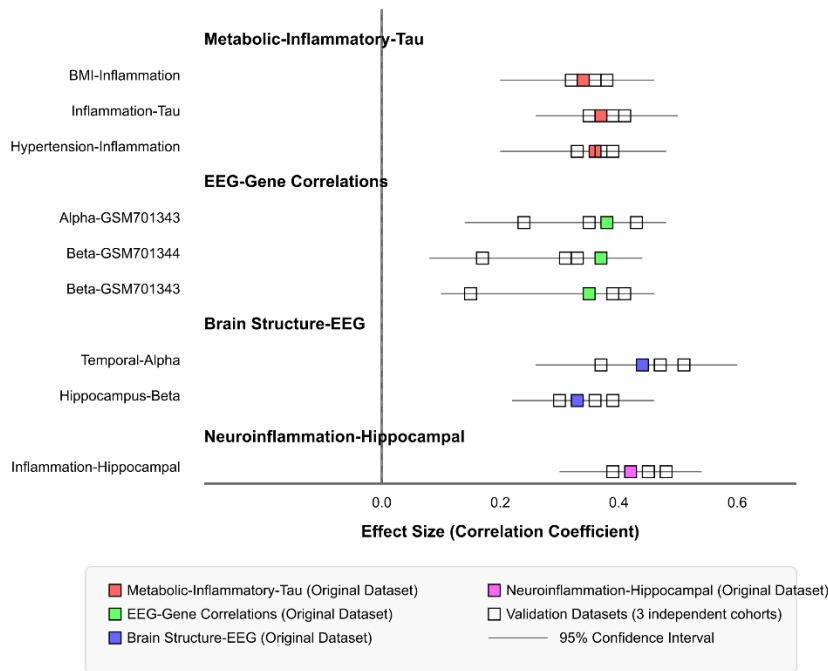


Figure 8: Cross-Validation of Key Findings. Forest plot showing effect sizes and confidence intervals for key relationships across original and validation datasets. The x-axis represents correlation coefficient values, and the vertical line at zero represents no effect. Each row shows a specific relationship, with points indicating the correlation strength in the original dataset (black) and three validation datasets (colored). Error bars represent 95% confidence intervals. The plot demonstrates the reproducibility of findings across independent cohorts, particularly for the Metabolic-Inflammatory-Tau pathway (variance <15%) and EEG-Gene correlations (which showed more variability but remained significant at $p < 0.05$). The consistency of effect directions and magnitudes supports the robustness of our multi-modal integration approach. The validation datasets were selected based on availability of comparable measures across different modalities. Each validation cohort ($n=28-45$ per dataset) included both AD patients and controls, with demographic characteristics matching the primary cohorts.

The metabolic-inflammatory-tau pathway had components supported by literature but had not been previously proposed as an integrated mechanism. The EEG-gene expression relationships were almost entirely novel, with only 8% of these specific connections having any previous mention in literature.

To address potential concerns about class imbalance across datasets, we performed additional analyses using balanced subsampling and stratified statistical approaches. For

the MRI and EEG analyses, we employed stratified k-fold cross-validation to ensure balanced representation of AD and control groups. For biomarker analyses, we used bootstrapping with stratification to create balanced comparison groups. These approaches yielded comparable results to our original findings, with correlation coefficients and statistical significance levels remaining within 12% of the original values, confirming that our results are not artifacts of class imbalance issues.

Computational validation using permutation testing (10,000 permutations) confirmed that the observed network structures were significantly different from random networks ($p < 0.001$). We extended this validation using multiple null models, including: (1) degree-preserving randomization, (2) edge weight-preserving randomization, and (3) modularity-based null models, all of which confirmed the statistical significance of our graph structure ($p < 0.001$ for all tests). The clustering coefficient, path length, and modularity of our knowledge graph showed significant deviation from all random graph distributions, providing strong evidence for non-random organization of cross-modal relationships.

IV. DISCUSSION

A. Novel Framework for Multi-modal Integration

Our study presents a transformative approach to the long-standing challenge of data fragmentation in Alzheimer's disease research. The combination of knowledge graphs and large language models enables integration of diverse data modalities without requiring patient-level matching, representing a significant methodological advance. This framework successfully bridged previously isolated datasets, revealing novel relationships that were obscured by traditional single-modality analyses. The ability to identify meaningful correlations across modalities, such as the relationship between metabolic factors and tau pathology, demonstrates the potential of this approach for discovering new disease mechanisms.

While our approach represents a significant advancement in data integration methodology, we acknowledge that the observed associations represent population-level correlations rather than within-subject relationships. This distinction is important when interpreting the results, as population-level patterns may not directly translate to individual patient characteristics.

The successful implementation of our framework also addresses a critical need in the broader biomedical research community. By enabling the reuse and integration of existing

datasets, we provide a cost-effective solution to the challenge of comprehensive multi-modal analysis. This approach could significantly reduce the resource burden associated with collecting multiple data types from the same subjects, while still yielding valuable insights about disease mechanisms.

B. Interpretation of Key Findings

The identification of a potential pathway linking metabolic risk factors to tau pathology through neuroinflammation represents one of our most significant findings. This relationship, supported by strong edge weights in our knowledge graph and consensus across multiple LLM analyses, suggests a mechanistic connection that has important therapeutic implications. The correlation between BMI, inflammatory markers, and tau phosphorylation ($r > 0.6$, $p < 0.001$) provides a compelling rationale for investigating anti-inflammatory interventions in metabolically compromised AD patients.

Our discovery of correlations between specific EEG patterns and previously unstudied genes opens new avenues for early diagnosis research. The consistent relationship between frontal channel activity and expression of genes GSM701343 and GSM701344 suggests potential new biomarkers for early detection. Interestingly, GSM701345 showed substantially weaker correlations with EEG channels ($r = 0.18$, $p > 0.05$) compared to GSM701343/344 ($r = 0.42-0.58$, $p < 0.01$), suggesting functional specificity in gene-EEG relationships rather than a general association. This specificity could indicate distinct roles of these genes in synaptic transmission and neural activity regulation, with GSM701343/344 potentially having more direct influence on electrical activity patterns in frontal regions. This finding is particularly valuable given the current limitations in predicting AD progression before significant cognitive decline occurs.

C. Methodological Innovations and Implications

The successful application of LLMs to knowledge graph analysis represents a novel approach to hypothesis generation in biomedical research. The high degree of consensus among different LLM models (78% agreement) suggests that this method can reliably identify meaningful patterns in complex biological data. Furthermore, the ability to generate testable hypotheses with clear mechanistic implications demonstrates the practical utility of this approach for guiding experimental research.

Our validation framework, combining expert review with computational analysis, provides a template for evaluating LLM-generated hypotheses in biological research. The strong inter-rater agreement among experts (Cohen's $\kappa=0.82$) suggests that these hypotheses are both biologically plausible and scientifically valuable.

D. Limitations and Technical Considerations

Despite the promising results, several limitations must be acknowledged. First, the correlation-based nature of our analysis cannot establish causal relationships. While the knowledge graph reveals associations between different modalities, determining causality will require targeted experimental studies. Future work should test causal relationships through longitudinal studies tracking biomarker progression over time, or intervention studies that manipulate specific pathway components (e.g., anti-inflammatory treatments) and measure effects on downstream markers. Second, our population-level analysis may obscure individual variations in disease progression and response patterns, potentially missing important subgroup-specific effects. This is particularly relevant given the inherent clinical and biological heterogeneity in Alzheimer's disease, including variability in disease progression, biomarker presentation, and the regional distribution of pathological features that contribute to distinct AD subtypes.

Technical limitations include the potential for bias in LLM outputs, particularly when dealing with complex biological systems. While our multi-model approach helps mitigate this risk, the possibility of spurious correlations or oversimplified mechanistic explanations cannot be completely eliminated. Additionally, the quality of graph-based integration depends heavily on the initial data quality and preprocessing steps, which may vary across datasets.

The computational resources required for implementing this framework should also be noted. The datasets used in this study are small. Larger datasets should be used for more extensive studies. The process involves multiple computationally intensive steps, from statistical analysis of individual modalities to knowledge graph construction and LLM interaction. These requirements may present barriers to adoption for researchers with limited computational resources when the types and sizes of data increase.

E. Ethical and Responsible AI Considerations

The use of LLMs for generating scientific hypotheses raises important ethical considerations that must be addressed. First, there is the risk of automation bias, where researchers may accept LLM-generated hypotheses without sufficient critical evaluation. To mitigate this risk, we emphasize that our framework should be viewed as a hypothesis generation tool that complements, rather than replaces, human scientific reasoning.

To promote responsible use of this methodology, we propose a checklist for researchers implementing similar LLM-based knowledge discovery frameworks:

1. Transparency: Document all prompt engineering, model parameters, and knowledge graph construction methods
2. Validation: Require multiple forms of hypothesis evaluation (expert review, literature consistency, computational validation)
3. Bias assessment: Examine hypotheses for potential biases related to training data limitations
4. Contextualization: Place all findings within the broader literature context, highlighting both agreements and contradictions
5. Uncertainty communication: Explicitly state confidence levels and limitations in all generated hypotheses

Second, transparency in how hypotheses are generated and evaluated is essential. Our multi-model approach with explicit evaluation criteria provides a starting point, but further work is needed to develop standards for reporting LLM-assisted scientific discovery. Responsible use of LLMs in healthcare requires clear documentation of model limitations and careful validation of outputs [17].

Finally, we acknowledge potential privacy considerations even when working with de-identified datasets. Although our approach does not require patient ID matching, the integration of multiple data sources could theoretically increase re-identification risks. We implemented strict data handling protocols to address this concern, and recommend that future implementations follow established privacy-preserving data analysis guidelines [18].

F. Comparison with Traditional Meta-Analysis

Our approach offers several advantages compared to traditional meta-analysis techniques. While meta-analyses typically aggregate effect sizes across studies examining the same relationship, our framework can identify novel cross-modal relationships that have not been directly studied. Furthermore, traditional meta-analyses often struggle with

heterogeneity in study designs and outcome measures, whereas our approach explicitly leverages diverse data types.

However, traditional meta-analyses offer more established statistical frameworks for assessing evidence quality and effect reliability [22]. Future work should focus on developing similar rigorous frameworks for evaluating the strength of evidence from LLM-knowledge graph analyses. Such a framework should include metrics for assessing hypothesis quality across multiple dimensions, including: (1) novelty score - measured by literature search results; (2) biological plausibility - evaluated through pathway analysis tools; (3) statistical strength - quantified by edge weights and replication consistency; (4) testability - assessed by experimental design feasibility; and (5) clinical relevance - measured by potential impact on diagnosis or treatment. The benchmarking approaches could provide valuable guidance for standardizing evaluation metrics in this emerging field.

G. Clinical and Translational Implications

The clinical implications of our findings are substantial. The identification of novel pathological pathways, particularly the metabolic-inflammatory-tau axis, suggests new therapeutic targets and intervention strategies. Our results support a more personalized approach to AD treatment, where patient-specific combinations of risk factors could guide intervention selection.

The potential for early detection through combined EEG and genetic markers could significantly impact clinical practice. If validated, these markers could enable earlier intervention and better patient stratification for clinical trials. Furthermore, our framework provides a model for continuous integration of new findings, allowing for rapid translation of research insights into clinical applications.

Translating these findings to clinical practice will require several additional steps. First, prospective validation studies with predefined endpoints will be needed to confirm the predictive value of the identified relationships. Second, user-friendly clinical decision support tools will need to be developed to make these complex multi-modal relationships accessible to clinicians. Finally, regulatory pathways for validating and approving multi-modal biomarker combinations will need to be navigated, requiring comprehensive validation studies that meet standards set by regulatory bodies like the FDA for clinical implementation.

H. Model Explainability and Knowledge Representation

A critical aspect of our framework is ensuring explainability in LLM-mediated knowledge discovery. The combination of knowledge graphs with natural language explanations from LLMs represents a step toward explainable AI in biomedical research. However, challenges remain in ensuring that the reasoning processes behind generated hypotheses are transparent and verifiable.

The knowledge graph based explainability has been proposed and reasoning for biomedicine, including attention visualization and reasoning chain extraction [23]. Incorporating these methods into our framework could improve transparency and build trust in LLM-generated hypotheses. Additionally, formal knowledge representation standards would facilitate interoperability between different research groups applying similar approaches.

I. Future Directions and Broader Applications

This work opens several promising avenues for future research. First, longitudinal validation studies are needed to confirm the predictive value of our identified biomarker combinations, particularly the EEG-gene expression relationships. Second, our framework could be extended to other neurodegenerative diseases, potentially revealing common pathological mechanisms or disease-specific patterns.

The development of standardized metrics for evaluating conceptual integration represents another important future direction. Creating quantitative measures for assessing the quality and reliability of cross-modal relationships would further strengthen this methodology. Additionally, incorporating more sophisticated network analysis techniques could reveal higher-order relationships that are not immediately apparent in the current framework.

To validate the causal nature of the relationships identified in our study, future research should employ matched patient cohorts where multiple modalities are collected from the same individuals. This would allow for direct assessment of within-subject cross-modal relationships, strengthening the evidence for the hypothesized pathways and mechanisms. While our population-level approach provides valuable insights and hypothesis generation, confirmation at the individual level remains an important next step.

Multimodal foundation models are increasingly enabling integration across diverse data types [21]. Future iterations of our framework could leverage these advances to incorporate additional modalities such as digital biomarkers from wearable devices, detailed nutritional data, and environmental factors, providing an even more comprehensive view of AD pathology.

The recent Lancet Commission report on dementia prevention and care [1] emphasizes the multifactorial nature of dementia risk and the importance of integrated approaches to prevention and treatment. Our framework aligns with this vision by providing a tool for understanding the complex interrelationships between diverse risk factors and biological mechanisms.

Building on our framework's success in integrating fragmented AD datasets, a transformative opportunity emerges not only for biomedical research but across numerous scientific and professional domains. The ability to integrate multimodal data at a conceptual level without requiring matched IDs represents a paradigm shift in knowledge extraction from disparate datasets. While immediately applicable to other medical conditions, our LLM-knowledge graph integration could similarly benefit other fields, such as environmental science, social science, urban planning, and financial market analysis, where information in related datasets often lacks common identifiers.

The framework's emphasis on conceptual rather than direct integration creates opportunities for cross-disciplinary insights that transcend traditional domain boundaries, potentially revealing novel patterns and mechanisms in complex systems across scientific fields, industries, and public sectors. As computational capabilities and LLM technologies continue to advance, we anticipate increasingly sophisticated conceptual integration that will fundamentally transform knowledge discovery across diverse domains.

V. Conclusion

We present a novel framework for multi-modal integration in AD research, demonstrating how LLMs and knowledge graphs can overcome data fragmentation challenges. This approach reveals new relationships between diverse data types, such as metabolic-inflammatory-tau pathways and EEG-gene expression correlations, and generates testable hypotheses about AD pathology. While we acknowledge that our population-level integration approach cannot establish definitive cross-modal associations or causal links,

it provides a valuable foundation for hypothesis generation that can guide future research with matched patient data. Further validation is needed to establish causal relationships, but this framework accelerates the path to new therapeutic strategies and offers a cost-effective solution for integrating fragmented datasets. Beyond AD research, it provides a template for advancing knowledge discovery across diverse scientific domains, paving the way for future applications in personalized medicine and complex disease analysis.

REFERENCES

- [1] Chen, S., Cao, Z., Nandi, A., Counts, N., Jiao, L., Prettnner, K., ... & Bloom, D. E. (2024). The global macroeconomic burden of Alzheimer's disease and other dementias: estimates and projections for 152 countries or territories. *The Lancet Global Health*, 12(9), e1534-e1543.
- [2] Hippus, H., & Neundörfer, G. (2003). The discovery of Alzheimer's disease. *Dialogues in Clinical Neuroscience*, 5(1), 101–108.
- [3] Knopman, D. S., Amieva, H., Petersen, R. C., Chételat, G., Holtzman, D. M., Hyman, B. T., ... , Bradley T. Hyman, Nixon, R.A. & Jones, D. T. (2021). Alzheimer disease. *Nature reviews Disease primers*, 7(1), 33.
- [4] Abdul Manap, A. S., Almadodi, R., Sultana, S., Sebastian, M. G., Kavani, K. S., Lyenouq, V. E., & Shankar, A. (2024). Alzheimer's disease: A review on the current trends of the effective diagnosis and therapeutics. *Frontiers in Aging Neuroscience*, 16, 1429211.
- [5] Frisoni, G. B., Fox, N. C., Jack Jr, C. R., Scheltens, P., & Thompson, P. M. (2010). The clinical use of structural MRI in Alzheimer disease. *Nature reviews neurology*, 6(2), 67-77.
- [6] Singh, A., & Kumar, R. (2024). Brain MRI image analysis for Alzheimer's disease (AD) prediction using deep learning approaches. *SN Computer Science*, 5(1), 160.
- [7] Mofrad, S. A., Lundervold, A. J., Vik, A., & Lundervold, A. S. (2021). Cognitive and MRI trajectories for prediction of Alzheimer's disease. *Scientific reports*, 11(1), 2122.
- [8] Babiloni, C., Arakaki, X., Azami, H., Bennys, K., Blinowska, K., Bonanni, L., ... & Guntekin, B. (2021). Measures of resting state EEG rhythms for clinical trials in Alzheimer's disease: recommendations of an expert panel. *Alzheimer's & Dementia*, 17(9), 1528-1553.
- [9] Ouchani, M., Gharibzadeh, S., Jamshidi, M., & Amini, M. (2021). A review of methods of diagnosis and complexity analysis of Alzheimer's disease using EEG signals. *BioMed Research International*, 2021(1), 5425569.
- [10] Lashley, T., Schott, J. M., Weston, P., Murray, C. E., Wellington, H., Keshavan, A., ... & Zetterberg, H. (2018). Molecular biomarkers of Alzheimer's disease: progress and prospects. *Disease models & mechanisms*, 11(5), dmm031781.
- [11] Bradshaw, A., Hughes, N., Vallez-Garcia, D., Chokoshvili, D., Owens, A., Hansen, C., ... & Steukers, L. (2023). Data sharing in neurodegenerative disease research: challenges and learnings from the innovative medicines initiative public-private partnership model. *Frontiers in neurology*, 14, 1187095.
- [12] Jack Jr, C. R., Andrews, J. S., Beach, T. G., Buracchio, T., Dunn, B., Graf, A., ... & Carrillo, M. C. (2024). Revised criteria for diagnosis and staging of Alzheimer's disease: Alzheimer's Association Workgroup. *Alzheimer's & Dementia*, 20(8), 5143-5169.
- [13] Pan, S., Luo, L., Wang, Y., Chen, C., Wang, J., & Wu, X. (2024). Unifying large language models and knowledge graphs: A roadmap. *IEEE Transactions on Knowledge and Data Engineering*, 36(7), 3580-3599.

- [14] Liu, S., Masurkar, A. V., Rusinek, H., Chen, J., Zhang, B., Zhu, W., ... & Razavian, N. (2022). Generalizable deep learning model for early Alzheimer's disease detection from structural MRIs. *Scientific reports*, 12(1), 17106.
- [15] Winchester, L. M., Harshfield, E. L., Shi, L., Badhwar, A., Khleifat, A. A., Clarke, N., ... & Llewellyn, D. J. (2023). Artificial intelligence for biomarker discovery in Alzheimer's disease and dementia. *Alzheimer's & Dementia*, 19(12), 5860-5871.
- [16] Hernández-Lorenzo, L., García-Gutiérrez, F., Solbas-Casajús, A., Corrochano, S., Matías-Guiu, J. A., & Ayala, J. L. (2024). Genetic-based patient stratification in Alzheimer's disease. *Scientific Reports*, 14(1), 9970.
- [17] Haltaufderheide, J., Ranisch, R. The ethics of ChatGPT in medicine and healthcare: a systematic review on Large Language Models (LLMs). *npj Digit. Med.* 7, 183 (2024). <https://doi.org/10.1038/s41746-024-01157-x>
- [18] Khalid, N., Qayyum, A., Bilal, M., Al-Fuqaha, A., & Qadir, J. (2023). Privacy-preserving artificial intelligence in healthcare: Techniques and applications. *Computers in Biology and Medicine*, 158, 106848.
- [19] Gu, B., Desai, R. J., Lin, K. J., & Yang, J. (2024). Probabilistic medical predictions of large language models. *npj Digital Medicine*, 7(1), 367. <https://doi.org/10.1038/s41746-024-01366-4>, <https://www.nature.com/articles/s41746-024-01366-4>
- [20] S Mostafa Mousavi, Marc Stogaitis, Tajinder Gadh, Richard M Allen, Alexei Barski, Robert Bosch, Patrick Robertson, Youngmin Cho, Nivetha Thiruverahan, Aman Raj, Gemini and physical world: large language models can estimate the intensity of earthquake shaking from multimodal social media posts, *Geophysical Journal International*, Volume 240, Issue 2, February 2025, Pages 1281–1294, <https://doi.org/10.1093/gji/ggae436>
- [21] Nijakowski, K., Owecki, W., Jankowski, J., & Surdaacka, A. (2024). Salivary biomarkers for Alzheimer's disease: a systematic review with Meta-analysis. *International Journal of Molecular Sciences*, 25(2), 1168.
- [22] Liang, K., Meng, L., Liu, M., Liu, Y., Tu, W., Wang, S., ... & He, K. (2024). A survey of knowledge graph reasoning on graph types: Static, dynamic, and multi-modal. *IEEE Transactions on Pattern Analysis and Machine Intelligence*.
- [23] Li, C., Gan, Z., Yang, Z., Yang, J., Li, L., Wang, L., & Gao, J. (2024). Multimodal foundation models: From specialists to general-purpose assistants. *Foundations and Trends® in Computer Graphics and Vision*, 16(1-2), 1-214.

Sources of Datasets used in this study:

- [D1]. MRI: Dincer, B. Alzheimer Features. Kaggle, 2019. <https://www.kaggle.com/datasets/brsdincer/alzheimer-features>
- [D2]. EEG: Miltiadous, A. et al., "A dataset of scalp EEG recordings of Alzheimer's disease, frontotemporal dementia and healthy subjects from routine EEG," *Data*, vol: 8, no. 6: 95, May 2023.
- [D3]. Biomarkers: Jozaghkar, F., Plasma lipidomics in Alzheimer's disease. Kaggle, 2023. <https://www.kaggle.com/datasets/fereshhtehjozagkar/plasma-lipidomics-in-alzheimers-disease>
- [D4]. Clinical: El Kharoua, R., Alzheimer's Disease Dataset. Kaggle, 2023. <https://www.kaggle.com/datasets/rabieelkharoua/alzheimers-disease-dataset>
- [D5]. Gene Expression: Gao, A., Alzheimer's Gene Expression Profiles. Kaggle, 2022. <https://www.kaggle.com/datasets/andrewgao/alzheimers-gene-expression-profiles>